

# Temperature Dependent Synthesis of Zinc Sulphide (ZnS) Nanoparticles and Its Characterization

Prabha Sharma<sup>1</sup>, Sujan Dhungana<sup>1</sup>, Rajan Rai<sup>1</sup>, Devendra Khadka<sup>2</sup>, Dipak Kumar Hitan<sup>3</sup>, Megh Raj Pokhrel<sup>4</sup>, Surendra Kumar Gautam<sup>1\*</sup>, Bhoj Raj Poudel<sup>1\*</sup>

<sup>1</sup>Department of Chemistry, Tri-Chandra Multiple Campus, Tribhuvan University, Kathmandu, Nepal

<sup>2</sup>Department of Chemistry, Tribhuvan Multiple Campus, Tribhuvan University, Tansen, Palpa, Nepal

<sup>3</sup>Department of Customs, Ministry of Finance, Kathmandu, Nepal

<sup>4</sup>Central Department of Chemistry, Tribhuvan University, Kathmandu, Nepal

\* Corresponding author: E-mail: surendra.gautam@trc.tu.edu.np; bhoj.poudel@trc.tu.edu.np

(Received: September 4, 2022, Received in revised form: November 15, Accepted: December 2, 2022, Available Online)

## Highlights

- Co-precipitation method is used for the synthesis of ZnS NPs.
- Ascorbic acid is used as capping agent.
- ZnS NPs are characterized by UV-Visible, FTIR, and XRD spectroscopy.
- ZnS NPs are found in cubic phase with zinc blend structure.
- Average particle sizes of ZnS NPs are 5.01 nm and 3.1 nm at 20 °C and 40 °C preparation temperature.

## Abstract

Zinc sulphide nanoparticles (ZnS NPs) were successfully synthesized by chemical co-precipitation method at 20°C and 40°C using zinc chloride ( $ZnCl_2$ ) and sodium sulphide ( $Na_2S$ ) as precursors. Ascorbic acid was used as a capping agent. The synthesized ZnS NPs were characterized by X-ray diffraction (XRD), UV-visible and Fourier transform infrared (FTIR) spectroscopy. UV-visible spectra showed that the bandgap of synthesized NPs was 3.8-3.9 eV at two different temperatures. XRD analysis showed the particles were present in the cubic phase with a zinc blend structure. FTIR spectra were used in the confirmation of the chemical species of the synthesized NPs. The average particle size calculated by using Debye-Scherrer's equation at 20°C and 40°C was found to be 5.01 and 3.1 nm which indicates that the particle size was temperature-dependent.

**Keywords:** ZnS NPs, XRD, FTIR, UV-visible spectroscopy, Debye Scherrer's equation

## Introduction

NPs are extremely small and ultrafine particles whose at least one dimension is less than 100 nm [1]. The properties of NPs strongly depend on their size and the three-dimensional confinement of the electrons [2-5]. Their size depends upon the surface-area-to-volume ratio. Particle size increases with an increase in surface-area-to-volume ratio thereby changing the physical as well as chemical properties of NPs [6,7]. Semiconductor NPs have been paid great attention due to their unique optical and electronic properties [8,9]. As one of the most important Group II-VI semiconductors; ZnS has been found in many applications like fluorescence probe [10], phosphorescence [11,12], biomedical [13,14], light-emitting diode (LED) [15], electroluminescent [16], non-linear optical devices [17] reflecting coatings [18], biosensing [19].

ZnS is an important Group II-VI semiconductor material for the development of various technologies and photovoltaic properties. It is an inorganic compound that exists in dual form. The two allotropic forms of ZnS NPs are cubic zinc blend with an energy

\*Corresponding author

gap in the range of 3.68 eV and wurtzite (hexagonal) with an energy gap in the range of 3.8 eV [20]. Many techniques have been developed for the synthesis of NPs such as chemical precipitation [21-24], sol-gel method [25], sonochemical method [26], microwave irradiation [27], colloidal microemulsion [5], spray pyrolysis [16], laser ablation technique [17], solvothermal synthesis [20], a soft chemical method [28] and so on.

It has been reported in most of the studies that temperature is the most prominent factor affecting the size of semiconductor NPs [29]. The scientific evidence revealed that at lower temperatures the size of nanoparticles was increased while at a higher temperature the size of NPs was decreased accordingly [30]. The literature survey provided the fact that high temperature is assisted in nucleation and low temperature is assisted in growth. The nucleation rate constant becomes larger with the increase in temperature while the growth rate constant becomes smaller with an increase in temperature [31]. That means the rate of nucleation is faster at high temperatures while the rate of growth is slower at high temperatures indicating smaller particle size at high temperatures.

There is strong evidence that bandgap energy increases with a decrease in particle size well illustrated by quantum confinement theory. This theory states that the potential well of the quantum box confines the holes in the valence band and the electrons in the conduction band. With shrinking particle size, this confinement of electrons and holes expands the bandgap energy between the valence band and conduction band [32].

Here, we investigated the impact of temperature on the optical and structural properties of ZnS NPs, synthesized by a simple chemical precipitation method, to optimize the condition of the precipitating process. For this, we reported the chemical precipitation of ZnS NPs and their characterization by UV-vis spectrometry, XRD, FTIR.

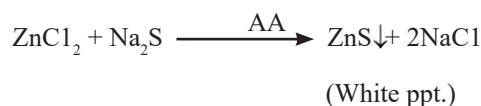
## Materials and Methods

### Materials

The synthesis method was quite straightforward and didn't call for any particular setup. ZnS was prepared from the reaction between precursor solutions i.e., ZnCl<sub>2</sub> and Na<sub>2</sub>S. None of the reactants needed additional purification and they were all of analytical grade. De-ionized water was used throughout the experiments.

### Synthesis of ZnS NPs

ZnS NPs were synthesized by chemical precipitation method using ZnCl<sub>2</sub> and Na<sub>2</sub>S as precursors and ascorbic acid (AA) was used as a capping agent. The synthesis was carried out at 20°C and 40°C temperatures. First of all, 0.01 M ZnCl<sub>2</sub> and 0.01 M ascorbic acid solution were mixed in a beaker followed by continuous stirring of the mixture using a magnetic stirrer. Then 0.01 M Na<sub>2</sub>S solution was added dropwise using the dropper, stirring the solution simultaneously till the formation of a white-colored solution. The solution was then allowed to settle for 24 hrs. and filtered, washed the precipitate (ppt) with double de-ionized water, and air-dried to get in powder form. The detailed methodology for the synthesis of ZnS NPs is shown in **Scheme 1**. The formation of ZnS NPs is represented by the following reaction [20, 33, 34].



**Scheme 1.** Synthesis of ZnS NPs

### Characterization of Synthesized NPs

The particle size and crystalline structure were determined by XRD. The average particle size (D) was determined by using Debye-Scherrer's equation calculating full width at half maximum (FWHM) from the XRD pattern obtained [24].

$$D = \frac{0.94 \times \lambda}{\beta \cos \theta}$$

Where  $\lambda$  denotes the wavelength of X-ray used (0.154 nm),  $\theta$  denotes the Bragg's angle, and  $\beta$  is the full width at half maximum in radian.

The absorption spectra were observed using UV-Visible spectroscopy between the range of 280-700 nm. The absorbance Vs

wavelengths plot gave the absorption maxima. The value of bandgap can be calculated by Tauc relation [35,36] which shows the relation between absorption coefficient ( $\alpha$ ) and the incident photon energy ( $h\nu$ ) and is represented as;

$$\alpha h\nu = A (h\nu - E_g)^{1/2}$$

Where  $\alpha$  denotes the absorption coefficient,  $h\nu$  denotes the incident photon energy,  $E_g$  is the bandgap energy, and A is constant.

The plot of  $(\alpha h\nu)^2$  versus  $h\nu$  gave the value of the bandgap by extrapolation of the linear region of the curve [23]. The vibrational structure of synthesized NPs at both temperatures was detected by FTIR [37]. Generally, FTIR is used to determine the characteristic functional group present on the surface of NPs that confirm the nanoscale properties of ZnS synthesized at different temperatures [38]. The different peaks obtained in the different regions were compared with the standard FTIR spectra.

## Results and Discussion

### XRD Analyses

The XRD (Rigaku ultima IV model) pattern was obtained using  $\text{CuK}\alpha$  radiations ( $\lambda = 1.514 \text{ \AA}$ ) for  $2\theta$  values ranging from  $10^\circ$  to  $90^\circ$  in synthesized ZnS NPs at two different temperatures as shown in Figure 1. The XRD pattern showed three diffraction peaks at  $2\theta$  values of  $28.58^\circ$ ,  $47.86^\circ$ , and  $56.61^\circ$  at  $20^\circ\text{C}$  while  $2\theta$  values of  $28.54^\circ$ ,  $47.81^\circ$ , and  $56.55^\circ$  at  $40^\circ\text{C}$  observed from (111), (220), and (311) planes, respectively which indicate that the particles were present in cubic phase with zinc blend structure (JCPDS card no. 05-0566) [39]. The peaks obtained well matched with the standard data as mentioned in [40] but are comparatively wider than that of bulk ZnS due to fine crystalline size. Since no other diffraction peaks were observed, it revealed that the synthesized ZnS NPs were pure. The (220) peak was used for the determination of average particle size. The average particle size of ZnS NPs was calculated from full width at half maximum (FWHM) of (220) peak using Debye-Scherrer's equation and was found to be 5.01 nm at  $20^\circ\text{C}$  and 3.1 nm at  $40^\circ\text{C}$  indicating a decrease in particle size with an increase in temperature. The decrease in particle size with an increase in temperature may be due to a slow rate of growth at high temperatures [31].

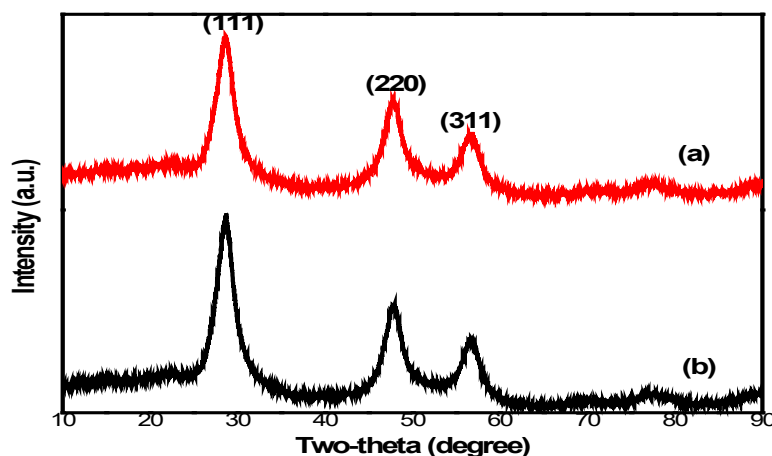


Fig 1. XRD pattern of synthesized ZnS samples at varying temperatures (a)  $20^\circ\text{C}$  and (b)  $40^\circ\text{C}$

### UV-Visible Analyses

Optical absorption spectra of ZnS NPs were measured using (SL 177 ELICO UV-Vis) spectrophotometer. The absorption spectra of NPs were measured in the range of 250–650 nm. The absorption edge of synthesized ZnS NPs at  $20^\circ\text{C}$  was found to be 330 nm and  $40^\circ\text{C}$  was found to be 315 nm as shown in Figure 2. The previous studies reported that the absorption edge of bulk ZnS was found to be 337 nm [41]. The absorption edge formed at 330 nm and 315 nm is lower than that of bulk ( $\sim 337 \text{ nm}$ ) which indicates a blue shift of absorption. The graph between  $(\alpha h\nu)^2$  Vs  $h\nu$  was plotted to calculate the band gap of synthesized ZnS NPs. The value of the bandgap was determined by extrapolating the straight portion of the curve of  $(\alpha h\nu)^2$  Vs  $h\nu$  on the  $h\nu$  axis as shown in Figure 3. The bandgap was found to be 3.8 eV and 3.9 eV for  $20^\circ\text{C}$  and  $40^\circ\text{C}$  which were higher than that of bulk ZnS ( $\sim 3.68 \text{ eV}$ ).

Using the effective mass approximation, the particle size was determined from the absorption data [41].

Where  $E_{g(\text{qd})}$  is the calculated bandgap of NPs and  $E_{g(\text{bulk})}$  is the bandgap of bulk ZnS,  $h$  is Planck's constant,  $m_h$  and  $m_e$  are the effective masses of hole and electron, respectively,  $r$  is the radius of NPs,  $e$  is the charge of the electron in C,  $\epsilon_0$  is the vacuum permittivity

constant and is the dielectric constant ( $\epsilon_s = 8.3$ ). The particle size obtained from this relationship was found to be 8.3 nm and 6.7 nm at 20°C and 40°C, respectively. Further, it was observed that with a decrease in particle size, the bandgap energy was increased. Thus, the result well agreed with the blue shift phenomena of bandgap due to quantum confinement of semiconductor NPs [32].

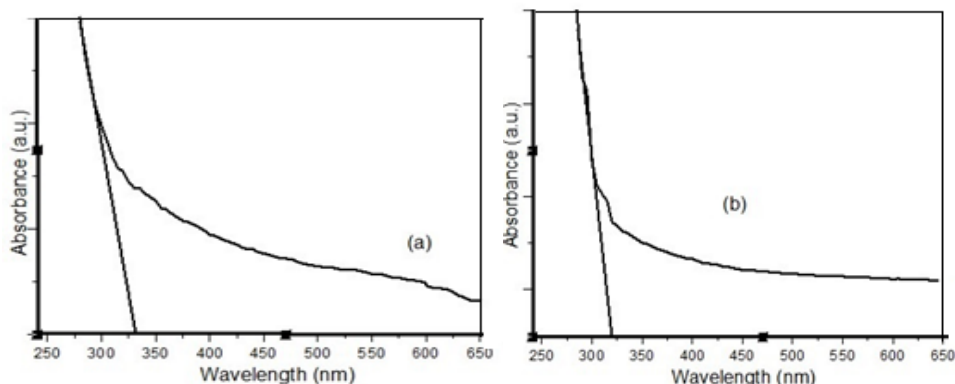


Fig 2. UV-Vis absorption spectra of the ZnS NPs prepared at different Temperatures (a) 20 °C and (b) 40 °C

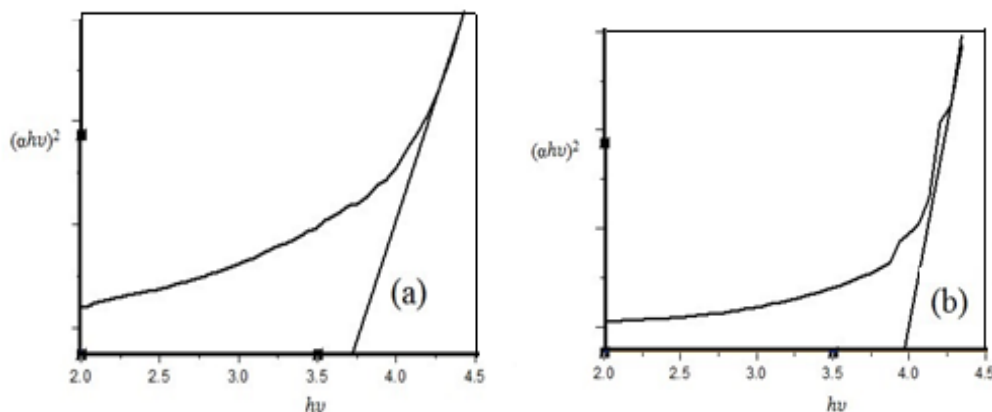


Fig 3.  $(\alpha h\nu)^2$  Vs  $h\nu$  plot to determine the bandgap of ZnS NPs at different temperatures (a) 20 °C and (b) 40 °C.

### FT-IR Analyses

The FT-IR spectra (IR AFFINITY-1 Shimadzu) of ZnS NPs at room temperature are shown in **Figure 4**. The FTIR spectra were recorded in the range of 400-4000  $\text{cm}^{-1}$ . The peaks were obtained due to different vibrational modes. The broad peak observed at 3186  $\text{cm}^{-1}$  was due to the absorption of water at the surface of NPs that indicate OH-stretching which well agreed with the reported value [37,41]. The peak observed at 1618  $\text{cm}^{-1}$  was due to C=O stretching modes [37,41]. The peaks observed at 1115  $\text{cm}^{-1}$  and 1001  $\text{cm}^{-1}$  were due to C-OH stretching mode [38]. The peak at 621  $\text{cm}^{-1}$  was due to Zn-S vibration which is in good agreement with the reported values [42].

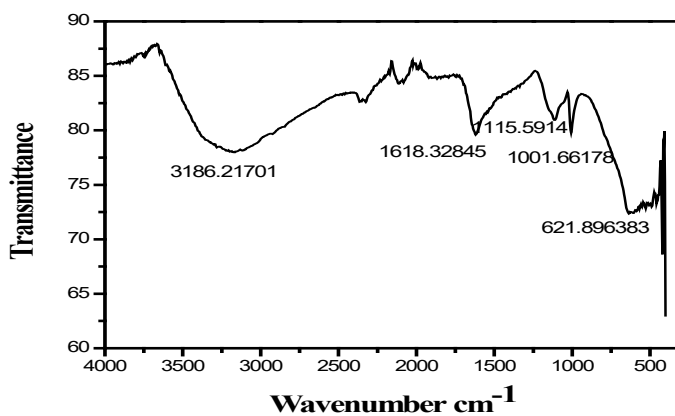


Fig 4. FTIR spectra of ZnS NPs at 20 °C

## Comparison of Different Methods for Synthesis of ZnS NPs

**Table 1** shows that the chemical precipitation method using  $ZnCl_2$  and  $Na_2S$  as precursors and ascorbic acid (AA) may be superior to other methods for the synthesis and characterization of ZnS NPs.

**Table 1.** Comparison of some methods of synthesis and characterization of ZnS NPs [43].

Method	Advantages	Disadvantages
Sol-Gel	High purity of the product	Need of well-controlled conditions Difficulty in preparation of precursor without cracking Longer reaction time
Sonochemical	High reaction yield	Need of ultrasonic radiation
Microwave irradiation	High purity of the product	Less accuracy of the control method on morphology and size
Chemical precipitation	Economic High reaction yield Simple method of working Suitable for large-scale production	Longer time for the product formation

## Applications of ZnS NPs

ZnS NPs are largely used in catalysis as they are chemically stable against hydrolysis and oxidation. ZnS is non-toxic and easily accessible, which makes it fit to be used as a catalyst in elimination of toxic and organic pollutants from water. Also, they are used as electrocatalysts for the direct conversion of ethyl alcohol in fuel cells [35]. Due to their wider band gap, better photostability, tunable and narrow emission, continuous absorption spectra, high flexibility, low cost, and good sensitivity, ZnS NPs are widely used as UV-sensors, chemical sensors, and biosensors [35-38]. ZnS NPs are also used as novel nano-modulators for plant growth [39].

## Conclusions

ZnS NPs were synthesized successfully at two different temperatures by the chemical co-precipitation method using ascorbic acid as a capping agent. XRD analysis confirmed the cubical phase of synthesized ZnS NPs. The particle size of synthesized NPs decreased from 5.01 nm to 3.1 nm as the temperature increased from 20 °C to 40 °C. The optical properties were determined by Uv-vis spectroscopy. The bandgap of synthesized NPs was 3.8 eV and 3.9 eV at 20 °C and 40 °C, respectively. The chemical bonding and vibrational modes of synthesized NPs were determined by FTIR. This study revealed that the size of synthesized ZnS NPs was found to be temperature-dependent and the bandgap, in turn, was particle size-dependent. The particle size was found to decrease with an increase in temperature meanwhile, the bandgap was increased with a decrease in particle size. All this evidence proved that ZnS NPs exhibit a strong quantum confinement effect with a blue shift in the band gap energy.

## Acknowledgments

The authors would like to acknowledge the Department of Chemistry, Tri-Chandra Campus for providing lab facilities and necessary materials. The authors are grateful to Dr. S.P. Singh (Nanotechnology and Advanced Materials Engineering, Sejong University, South Korea) for XRD analysis.

## Reference

1. P. Christian, F. Von Der Kammer, M. Baalousha, and T. Hofmann, Nanoparticles: Structure, Properties, Preparation and Behaviour in Environmental Media, *Ecotoxicology*, (2008), 17(5), 326–343. (DOI: <https://doi.org/10.1007/s10646-008-0213-1>).
2. A. Henglein, Small-Particle Research: Physicochemical Properties of Extremely Small Colloidal Metal and Semiconductor Particles, *American Chemical Review*, (1989), 89(8), 1861–1873. (DOI: <https://doi.org/10.1021/Cr00098a010>).

3. Y. Wang and N. Herron, Nanometer-Sized Semiconductor Clusters: Materials Synthesis, Quantum Size Effects, and Photophysical Properties, *The Journal of Physical Chemistry*, (1991), 95(2), 525–532. (DOI: <https://doi.org/10.1021/j100155a009>).
4. H. Weller, Quantized Semiconductor Particles: A Novel State of Matter for Materials Science, *Advanced Materials*, (1993), 5(2), 88–95. (DOI: <https://doi.org/10.1002/Adma.19930050204>)
5. A. P. Alivisatos, Semiconductor Clusters, Nanocrystals, and Quantum Dots, *Science*, (1996), 271, 933–937. (DOI: <http://doi.org/10.1126/Science.271.5251.933>).
6. K. W. Powers, M. Palazuelos, B. M. Moudgil, and S. M. Roberts, Characterization of The Size, Shape and State of Dispersion of Nanoparticles for Toxicological Studies, *Nanotoxicology*, (2007), 1(1), 42–51. (DOI: <https://doi.org/10.1080/17435390701314902>).
7. B. Regmi, T. R. Binadi, S. N. Jha, R. K. Chaudhary, B. R. Poudel, and S. K. Gautam, Antibacterial and Antioxidant Studies of Green Synthesized Silver Nanoparticles Using Azadirachta Indica (Neem) Leaf Extract, *International Journal of Applied Sciences and Biotechnology*, (2021), 9(3), 220–226. (DOI: <http://doi.org/10.3126/Ijasbt.V9i3.39069>).
8. M. Wadhvani and S. Jain, Synthesis and Antimicrobial Activity of Zinc Sulphide Nanoparticles, *Research Journal of Recent Sciences*, (2015), 4, 36–39.
9. S. Dhungana, B. R. Poudel, and S. K. Gautam, Synthesis and Characterization of ZnTe Nanoparticles, *Nepal Journal of Science and Technology*, (2016), 17(1), 1–3. (DOI: <https://doi.org/10.3126/Njst.V17i1.25054>).
10. Y. Li, J. Chen, C. Zhu, L. Wang, D. Zhao, S. Zhuo, and Y. Wu, Preparation and Application of Cysteine-capped ZnS Nanoparticles as Fluorescence Probe in the Determination of Nucleic acids, *Spectrochemical Acta Part A: Molecular and Biomolecular Spectroscopy*, (2004), 60(8–9), 1719–1724. (DOI: <https://doi.org/10.1016/J.Saa.2003.09.012>).
11. Y. Li, L. Zhang, K. Kisslinger, and Y. Wu, Green Phosphorescence of Zinc Sulfide Optical Ceramics, *Optical Materials Express*, (2014), 4(6), 1140. (DOI: <https://doi.org/10.1364/OME.4.001140>).
12. H. W. Liu, I. R. Laskar, C. P. Huang, J. A. Cheng, S.S. Cheng, L. Y. Luo, H.R. Wang, and T. M. Chen, Enhanced Phosphorescence and Electroluminescence in Triplet Emitters by Doping Gold into Cadmium Selenide/Zinc Sulfide Nanoparticles, *Thin Solid Films*, (2005), 489(1–2), 296–302. (DOI: <https://doi.org/10.1016/J.Tsf.2005.04.094> ).
13. K. Pathakoti, H. M. Hwang, H. Xu, Z. P. Aguilar, and A. Wang, In Vitro Cytotoxicity of CdSe/ZnS Quantum Dots with Different Surface Coatings to Human Keratinocytes Hacat Cells, *Journal of Environmental Sciences (China)*, (2013), 25(1), 163–171. (DOI: [https://doi.org/10.1016/S1001-0742\(12\)60015-1](https://doi.org/10.1016/S1001-0742(12)60015-1)).
14. P. Kumar, S. Maikap, K. Singh, S. Chatterjee, Y. Y. Chen, H. M. Cheng, R. Mahapatra, J. T. Qiu, and J. R. Yang, Highly Reliable Label-Free Detection of Urea/Glucose and Sensing Mechanism Using SiO<sub>2</sub> and CdSe-ZnS Nanoparticles in Electrolyte-Insulator-Semiconductor Structure, *Journal of Electrochemical Society*, (2016), 163(13), B580–B587. (DOI: <https://doi.org/10.1149/2.0331613jes>)
15. H. Kim, J. Y. Han, D. S. Kang, S.W. Kim, D. S. Jang, M. Suth, A. Kirakosyan, and D. Y. Jeon, Characteristics of CuInS<sub>2</sub>/ZnS Quantum Dots and its Application on LED, *Journal of Crystal Growth*, (2011), 326(1), 90–93. (DOI: <https://doi.org/10.1016/J.Jcrysgr.2011.01.059>).
16. C. Falcony, M. Garcia, A. Ortiz, and J. C. Alonso, Luminescent Properties of ZnS: Mn Films Deposited by Spray Pyrolysis, *Journal of Applied Physics*, (1992), 72(4), 1525–1527. (DOI: <https://doi.org/10.1063/1.351720>).
17. K. Vasudevan, M. C. Divyasree, and K. Chandrasekharan, Enhanced Nonlinear Optical Properties of ZnS Nanoparticles in 1D Polymer Photonic Crystal Cavity, *Optics and Laser Technology*, (2019), 114, 35–39. (DOI: <https://doi.org/10.1016/J.Optlastec.2019.01.027>).
18. S. Kumar, N. K. Verma, and M. L. Singla, Diffuse Reflectance and Reflective Flexible Coatings of Capped ZnS Nanoparticles, *Materials Chemistry and Physics*, (2013), 142(2–3), 734–739. (DOI: <https://doi.org/10.1016/J.Matchemphys.2013.08.032>).
19. G. Suganthi, G. Ramanathan, T. Arockiadoss, and U. T. Sivagnanam, Facile Synthesis of Chitosan-Capped ZnS Nanoparticles as a Soft Biomimetic Material in Biosensing Applications, *Process Biochemistry*, (2016), 51(7), 845–853. (DOI: <https://doi.org/10.1016/J.Procbio.2016.04.001>).

20. Y. Yesu Thangam, R. Anitha, and B. Kavita, Novel Method to Synthesize and Characterize Zinc Sulfide Nanoparticles, *International Journal of Applied Sciences and Engineering Research*, (2012), 1(2), 282–286. (DOI: <https://doi.org/10.6088/ijaser.0020101029>).
21. S. M. Scholz, R. Vacassy, J. Dutta, H. Hofmann, and M. Akinc, Mie Scattering Effects from Monodispersed ZnS Nanospheres, *Journal of Applied Physics*, (1998), 83(12), 7860–7866. (DOI: <https://doi.org/10.1063/1.367961>).
22. J. Nanda, S. Sapra, D. D. Sarma, N. Chandrasekharan, and G. Hodes, Size-Selected Zinc Sulphide Nanocrystallites: Synthesis, Structure, and Optical Studies, *Chemistry of Materials*, (2000), 12(4), 1018–1024. (DOI: <https://doi.org/10.1021/Cm990583f>).
23. H. A. T. Al-Ogaili, Synthesis of Colloidal Zinc Sulfide Nanoparticle Via Chemical Route and Its Structural and Optical Properties, *International Journal of Advanced Research in Science, Engineering and Technology*, (2016), 3(3), 1587–1592.
24. N. K. Abbas, K. T. Al-Rasoul, and Z. J. Shanan, New Method of Preparation ZnS Nano Size at Low P<sup>H</sup>, *International Journal of Electrochemical Science*, (2013), 8(2), 3049–3056. [Online]. Available: [www.Electrochemsci.Org](http://www.Electrochemsci.Org).
25. B. Bhattacharjee, D. Ganguli, K. Iakoubovskii, A. Stesmans, and S. Chaudhuri, Synthesis and Characterization of Sol-Gel Derived ZnS: Mn<sup>2+</sup> Nanocrystallites Embedded in a Silica Matrix, *Bulletin of Material Science*, (2002), 25(3), 175–180. (DOI: <https://doi.org/10.1007/BF02711150>).
26. H. Qin, T. Hu, Y. Zhai, N. Lu, and J. Aliyeva, Sonochemical Synthesis of ZnS Nanolayers on the Surface of Microbial Cells and their Application in the Removal of Heavy Metals, *Journal of Hazardous Materials*, (2000), 400(123161), 1-11. (DOI: <https://doi.org/10.1016/J.Jhazmat.2020.123161>).
27. M. V. Limaye, S. Gokhale, S. A. Acharya, and S. K. Kulkarni, Template-Free ZnS Nanorod Synthesis by Microwave Irradiation, *Nanotechnology*, (2008), 19(41), 1–5. (DOI: <https://doi.org/10.1088/0957-4484/19/41/415602>).
28. I. S. Popov, N. S. Kozhevnikova, M. A. Melkozerova, A. S. Vorokh, and A. N. Enyashin, Nitrogen-Doped ZnS Nanoparticles: Soft-Chemical Synthesis, EPR Statement and Quantum-Chemical Characterization, *Materials Chemistry and Physics*, (2018), 215, 176–182. (DOI: <https://doi.org/10.1016/J.Matchemphys.2018.04.115>).
29. A. Mohammed Fayaz, K. Balaji, P. T. Kalaichelvan, and R. Venkatesan, Fungal Based Synthesis of Silver Nanoparticles- An Effect of Temperature on the Size of Particles, *Colloids and Surfaces B: Biointerfaces*, (2009), 74(1), 123–126 (DOI: <https://doi.org/10.1016/J.Colsurfb.2009.07.002>).
30. M. M. H. Khalil, E. H. Ismail, K. Z. El-Baghdady, and D. Mohamed, Green Synthesis of Silver Nanoparticles using Olive Leaf Extract and its Antibacterial Activity, *Arabian Journal of Chemistry*, (2014), 7(6), 1131–1139. (DOI: <https://doi.org/10.1016/J.Arabjc.2013.04.007>).
31. H. Liu, H. Zhang, J. Wang, and J. Wei, Effect of Temperature on the Size of Biosynthesized Silver Nanoparticle: Deep Insight into Microscopic Kinetics Analysis, *Arabian Journal of Chemistry*, (2020), 13(1), 1011–1019. (DOI: <https://doi.org/10.1016/j.arabjc.2017.09.004>).
32. M. Singh, M. Goyal, and K. Devlal, Size and Shape Effects on the Band Gap of Semiconductor Compound Nanomaterials, *Journal of Taibha University for Science*, (2018), 12(4), 470–475. (DOI: <https://doi.org/10.1080/16583655.2018.1473946>).
33. K. Winkelmann, T. Noviello, and S. Brooks, Preparation of CdS Nanoparticles by First-Year Undergraduates, *Journal of Chemical Education*, (2007), 84(4), 709–710. (DOI: <https://doi.org/10.1021/ed084p709>).
34. K. Ashwini, Yashaswini, and C. Pandurangappa, Solvothermal Synthesis, Characterization, and Photoluminescence Studies of ZnS: Eu Nanocrystals, *Optical Materials*, (2014), 37, 537–542. (DOI: <https://doi.org/10.1016/j.optmat.2014.07.019>).
35. S. Baset, H. Akbari, H. Zeynali, and M. Shafie, Size Measurement of Metal and Semiconductor Nanoparticles Via UV-Vis Absorption Spectra, *Digest Journal of Nanomaterial Biostructure*, (2011), 6(2), 709–716.
36. A. Bhujel, B. Sapkota, R. L. Aryal, B. R. Poudel, S. Bhattarai, and S. K. Gautam, Insight of Precursor Concentration, Particle Size and Band Gap of Zirconia Nanoparticles Synthesized by Co-Precipitation Method, *Bibechana*, (2021), 18(1), 1–9. (DOI: <https://doi.org/10.3126/bibechana.v18i1.28958>).

37. M. Sathishkumar, M. Saroja, M. Venkatachalam, and M. Senthilkumar, Antimicrobial Activity of Zinc Sulphide Nanoparticles and to Study their Characterization, *Elixir Electrical Engineering*, (2016), 101, 44118–44121.
38. P. Suganya and P. U. Mahalingam, Green Synthesis and Characterization of Zinc Sulphide Nanoparticles from Macro Fungi Pleutrous Florida, *IOSR Journal of Applied Chemistry*, (2017), 10(7–3), 37–42. (DOI: <https://doi.org/10.9790/5736-1007033742>).
39. S. Biswas and S. Kar, Fabrication of ZnS Nanoparticles and Nanorods with Cubic and Hexagonal Crystal Structures: A Simple Solvothermal Approach, *Nanotechnology*, (2008), 19(4), 1–11. (DOI: <https://doi.org/10.1088/0957-4484/19/04/045710>).
40. M. Ahmad, K. Rasool, Z. Imran, M. A. Rafiq, and M. M. Hasan, Structural and Electrical Properties of Zinc Sulfide Nanoparticles, *Saudi International Electronics, Communications and Photonics Conference (SIECPC)*, (2011), 1-4. (DOI: <https://doi.org/10.1109/SIECPC.2011.5876907>).
41. P. Iranmanesh, S. Saeednia, and M. Nourzpoor, Characterization of ZnS Nanoparticles Synthesized by Co-Precipitation Method, *Chinese Physics B*, (2015), 24(4), 46104-1-046104-4. (DOI: <https://doi.org/10.1088/1674-1056/24/4/046104>).
42. V. D. Mote, Y. Purushotham, and B. N. Dole, Structural, Morphological and Optical Properties of Mn Doped ZnS Nanocrystals, *Ceramica*, (2013), 59(351), 395–400. (DOI: <https://doi.org/10.1590/S0366-69132013000300008>)
43. R. P. Dewi, A. Nurdiana, L. Astuti, R. Ragadita, and A. B. D. Nandiyanto, Review: Synthesis of Zinc Sulfide Nanoparticles by Various Methods, *Arabian Journal of Chemical and Environmental Research*, (2021), 08(02), 355-371.
44. H. Naeimi, F. Kiani, and M. Moradian, ZnS Nanoparticles as an Efficient and Reusable Heterogeneous Catalyst for Synthesis of 1-substituted-1H-tetrazoles Under Solvent-free Conditions, *Journal of Nanoparticle Research*, (2014), 16(09). (DOI: 10.1007/s11051-014-2590-0).
45. X. Fang, Y. Bando, U. K. Gautam, T. Zhai, H. Zeng, X. Xu, M. Liao, and D. Golberg, ZnO and ZnS nanostructures: Ultraviolet-light emitters, lasers, and sensors, *Critical Reviews in Solid State and Materials Sciences*, (2009), 34(3-4), 190-223. (DOI: 10.1080/10408430903245393).
46. X. Wang, Z. Xie, H. Huang, Z. Liu, D. Chen, and G. Shen, Gas Sensors, Thermistor and Photodetector Based on ZnS Nanowires, *Journal of Materials Chemistry*, (2012), 22(14), 6845–6850. (DOI: 10.1039/c2jm16523f).
47. F. Zhang, C. Li, X. Li, X. Wang, Q. Wan, Y. Xian, L. Jin, and K. Yamamoto, ZnS Quantum Dots Derived a Reagent less Uric Acid Biosensor, *Talanta*, (2006), 68(4), 1353–1358. (DOI: 10.1016/j.talanta.2005.07.051).
48. B. N. Aini, S. Siddiquee, K. Ampon, K. F. Rodrigues, and S. Suryani, Development of Glucose Biosensor Based on ZnO Nanoparticles Film and Glucose Oxidase-immobilized Eggshell Membrane, *Sensing and Bio-Sensing Research*, (2015), 4, 46–56. (DOI: 10.1016/j.sbsr.2015.03.004).
49. M. Thapa, M. Singh, C. K. Ghosh, P. K. Biswas, and A. Mukherjee, Zinc Sulphide Nanoparticle (ZnS): A Novel Nano-modulator for Plant Growth, *Plant Physiology and Biochemistry*, (2019), 142, 73–83. (DOI: 10.1016/j.plaphy.2019.06.031).